Reaction of Sn-Bearing Solders with Nickel-based Under Bump Metallisations

G. Qi, M. He and Z. Chen

Abstract – This work relates to wafer bumping technologies for flip chip packaging applications in the electronics industry. Nickel and its alloys are alternative under bump metallization (UBM) materials because of their slower reaction rates with Sn-based solder as compared to Cu-based UBMs. In this study, we compared the morphologies of the intermetallic compounds (IMC) formed between Sn-bearing solders (Sn3.5Ag and eutectic Sn-Pb) and two types of nickel-based UBMs, electroless Ni-P (EN) and sputtered nickel. Both chunky-type and needle-type of intermetallics were observed between the EN UBM and the solders. In the case of sputtered Ni UBM, there is only a layer of scallop-type intermetallics formed. The morphology change and growth kinetics of the IMC in thermal aging process were analysed. Kirkendall voids were noticed from samples of Sn3.5Ag solder vs Ni-P UBM that have undergone prolonged thermal aging at high temperature.

Keywords: Intermetallics, Solder, UBM, Packaging, Flip-chip

1 BACKGROUND

Flip chip technology has been proving itself to be a viable high performance and high I/O density packaging solution in the electronics industry [1-3]. In this new packaging approach, metallic bumps are built on the chip's I/O pads via wafer bumping processes. When the chip is 'flipped over' and attached to a matching pattern on a substrate, the bumps provide the interconnection, which is otherwise conventionally achieved by wire bonding. Among the various bump materials involved in flip chip packaging, solders have been most commonly used. To build solder bumps on IC pads, intermediate layers, commonly called under bump metallization (UBM), of suitable materials must be used to achieve the required adhesion and reliability because of the mismatch between solders and IC I/O pad metallization. The selection and performance of the UBMs have been the topic of many studies [4-5].

Historically, Cr-Cu UBM was successfully used in the IBM C-4 technology where high lead content Sn-Pb solder was the bump material. Challenges arose when a similar flip chip structure was used in chip-on-board applications where low-temperature solders are necessary to avoid thermal degradation of the substrates. The most popular solder has been the eutectic tin-lead system which has a melting temperature of 183°C. Recently, lead-free solders are used to replace the Pb-bearing solders because of environmental concerns. A common feature of these low melting solders is their high Sn content compared with the high-lead solder in the IBM C4 technology. These solders were found to be incompatible with the Cr-Cu UBM due to rapid spalling of Cu-Sn intermetallic compounds [4-7]. As alternatives, nickel-based UBMs, such as electrolessly plated Ni-P alloy (EN) and sputtered nickel, have attracted attention because of their fairly good wettability [8] and slow reaction rate with solders [9]. Many studies have been devoted to the understanding of the interactions between the Sn-based solders with Ni-P and sputtered nickel UBMs [4-5]. The information published so far suggests that nickel-based UBMs could form intermetallic compounds (IMCs) with the popular tin-based solders (be they lead-bearing or lead-free). With different solder and UBM combinations, differences are expected with respect to the types of IMCs formed, the interfacial morphology, their growth rate under reflow and annealing conditions, and their mechanical and electrical integrity. Such differences can ultimately lead to differences in the reliability of the final products.

SIMTech has started R&D activities on wafer bumping since about six years ago. We have been working on various process developments with respect to bumping with different materials, including eutectic Sn-Pb solders, high-lead solders, lead-free solders, electroless nickel and gold. Materials selection for the UBMs for different bump materials is always an important part of consideration for achieving good reliability of the whole bump system. We have been using sputtered pure nickel as well as electroless nickel as the UBMs for our solder bumps. The work presented in this report is a contiuation of our effort on gaining more understanding of the interaction between solders and nickel based UBM systems.

2 OBJECTIVE

In this work, we compare the interaction of two Sn-bearing solders (96.5Sn3.5Ag and eutectic Sn-Pb) with two types of nickel-based under bump metallizations (EN and sputtered pure Ni). These materials were chosen based on the following considerations: The Sn3.5Ag solder is one of the popular lead-free solder systems and the eutectic Sn-Pb is still the most widely used solder in the industry. EN UBM is gaining popularity in industry because of its simplicity in manufacturing processes. On the other hand, sputtered nickel is preferred in certain situations where a continuous film is required for bump build-up by electroplating. The morphology of IMCs formed under a given set of reflow and annealing conditions was observed. The growth kinetics of the IMC were assessed and compared.

3 EXPERIMENTAL

The substrates used in this study were prepared from blank wafers. Silicon wafers with 5000-Å-thick silicon oxide were cleaned by soaking in pure nitric acid at room temperature for 3 min, followed by rinsing with de-ionized water, blow drying with pure nitrogen and oven baking at 150°C for half an hour. The sputtered nickel UBM was prepared by sputtering a chromium layer of about 3000 Å thick first, followed by nickel sputtering using pure nickel targets. The chromium provides good adhesion of the UBM to the wafer or aluminum metallization and also functions as a diffusion barrier to the solder elements to the metallizations below it, as in a real bumping application. The thickness of the sputtered nickel is about 1 μm. Finally, a thin layer of pure gold was sputtered to provide protection of nickel from oxidation.

The Ni-P UBM was obtained by electrolessly plating Ni on the above mentioned sputtered nickel substrate. Before the plating, the sputtered gold layer was etched away. After reaching a thickness of about 5 μm the plating was stopped and a final finish by immersion gold was applied as a surface protection.

In a reflow experiment, a few grams of flux-core solder wire was placed on the substrate and then sent into a reflow oven. Three thermocouples, two attached to the bottom of the sample and one fixed on the oven ceiling were used to monitor the temperature change during the reflow process. The temperature profiles were controlled such that the solder was heated to a peak temperature 30 degrees above their respective melting temperature (251°C for Sn3.5Ag and 213°C for eutectic Sn-Pb), sat full oven heating capacity (it took ~ 4 min for eutectic Sn-Pb and ~ 6 min for Sn3.5Ag) and cooled down in the oven to a temperature below their melting points. The sample was then taken out of the oven and cooled down in the ambient condition. The reflow process kept the solders above their melting temperatures for about 1 min for eutectic Sn-Pb and 2 min for Sn3.5Ag.

The reflowed samples were further prepared for observations on the cross sectional structure and top view of the morphology of the IMCs. Standard metallography practice was followed to reveal the cross sectional microstructure. To observe the top view of the IMCs, a specimen was ground first to remove most of the solder. The remaining solder was etched away with 2% HCl followed by through rinsing with DI water and blow drying with nitrogen. The specimen was then examined using scanning electron microscope (SEM) and energy dispersive X-ray (EDX) analysis.

Selected samples were thermally aged at predetermined temperatures (130, 150, 170 and 190°C) for prolonged period in air. The samples were further prepared as described above to observe the morphology change and growth of the IMCs.

4 RESULTS

4.1 Morphology of IMC in as-reflowed samples

Fig. 1 shows typical views of the intermetallics formed by reflowing the two solders on electroless Ni-P film. The difference in the IMC morphologies between the two solder systems is clearly seen. Fig. 1(a) shows that the intermetallics formed between Sn3.5Ag solder and Ni-P film exists in both chunky blocks with clearly visible crystal facets and irregular-shaped small crystal agglomerates, while the IMCs of the eutectic Sn-Pb solder with Ni-P Fig. 1(c) exhibit similar forms but the size is much smaller. The faceted grains are less obvious compared to the ones with Sn3.5Ag solder but are still clearly visible. EDX analysis showed that the elemental composition of intermetallics observable in Figs. 1(a) and 1(c) is Ni_3Sn_4, irrespective of their shape and sizes. This is in agreement while the intermetallics of the Sn-Pb system appears to be discontinuous with a lot of needle-like spikes Fig. 1(d).

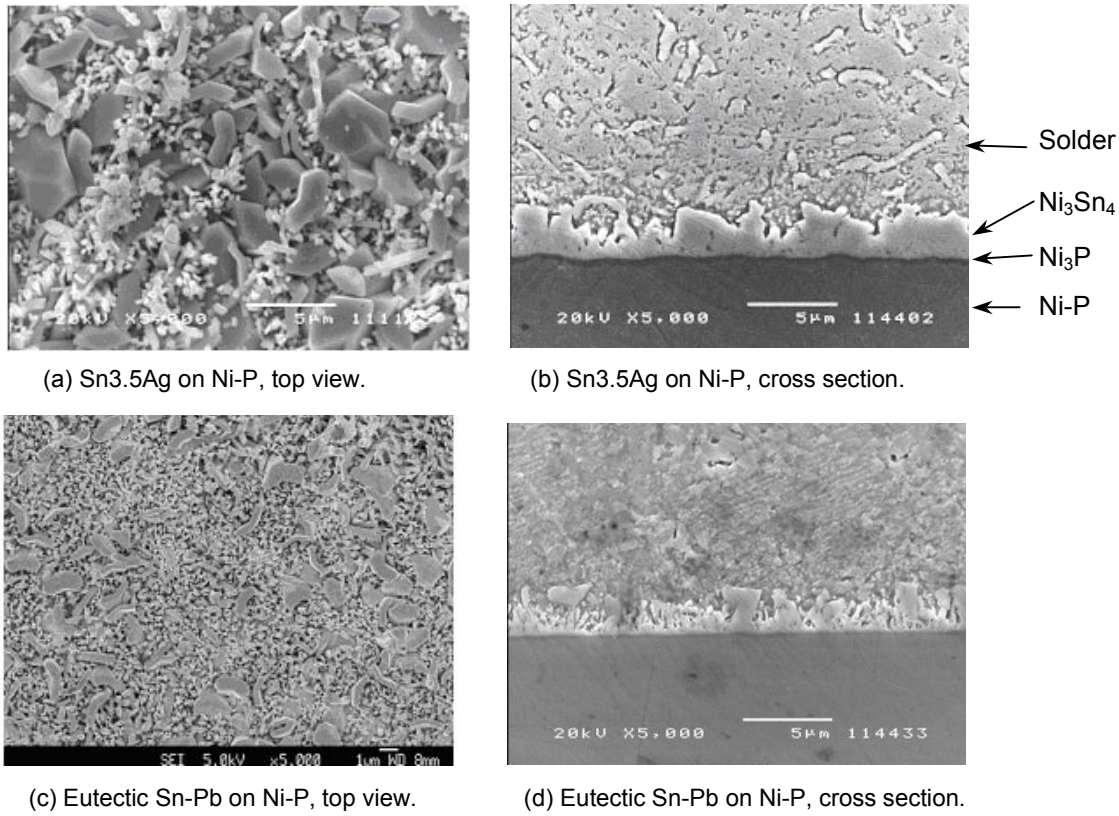

(a) Sn3.5Ag on Ni-P, top view.

(b) Sn3.5Ag on Ni-P, cross section.

(c) Eutectic Sn-Pb on Ni-P, top view.

(d) Eutectic Sn-Pb on Ni-P, cross section.

Fig. 1. Top and cross sectional views of the intermetallic compounds formed between Sn3.5Ag and eutectic Sn-Pb solders and electroless Ni-P alloy UBM.

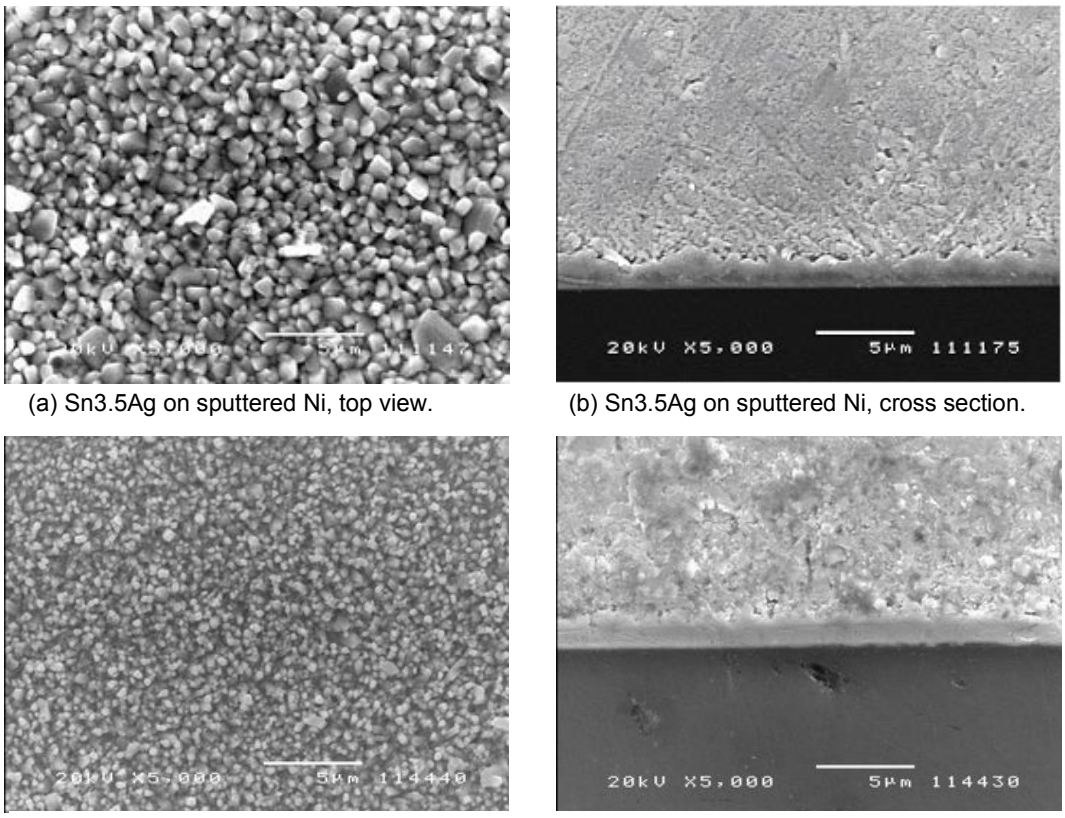

(a) Sn3.5Ag on sputtered Ni, top view.

(b) Sn3.5Ag on sputtered Ni, cross section.

(c) Sn-Pb on sputtered Ni, top view.

(d) Sn-Pb on sputtered Ni, cross section.

Fig. 2. Top and cross sectional views of the intermetallic compounds formed between Sn3.5Ag and eutectic Sn-Pb solders and sputtered nickel UBM after reflow.

with what was reported by Jang *et al*. [10,11] and Jeon *et al.* [12]. A continuous rough intermetallic layer is observed from the cross sectional view of the Sn3.5Ag sample Fig. 1(b), EDX analysis of the cross sections of the samples confirmed that in between the Ni_3Sn_4 and Ni-P film there exists of a P-rich layer. This layer is clearly visible from the cross sectional micrograph in Fig. 1(b). Jang *et al*. [11] confirmed that the crystal structure of such layer was Ni_3P and they attributed its formation to the assistance from Ni_3Sn_4 formation.

The top and cross sectional morphologies of the IMCs formed between the two solders and sputtered Ni film are shown in Fig. 2. Although the composition of the IMCs formed by the two solders with Ni film is the same as with the Ni-P alloy, the Ni_3Sn_4 grains are all scallop shaped. The IMC grains of the Sn3.5Ag system appear much larger than those of the Sn-Pb system but in both systems the grain sizes are quite uniform. The interfaces between the IMC and Ni film are relatively straight compared with the Ni-P UBM combinations.

4.2 Growth of the IMC during thermal aging

The reaction of the solders with the Ni-based UBMs continues during the thermal aging. This is evidenced by the increase of the thickness and larger grain sizes of the IMCs compared to the as-reflowed samples.

Ni-P UBM. Fig. 3 shows typical views of the Sn3.5Ag with Ni-P combination after annealing at 170°C for 100 hours. The IMC layer thickness and grain size varies with the aging temperature and time. Similar morphologies were also observed from the eutectic Sn-Pb and Ni-P combination. The small IMC crystal agglomerates, as seen in Fig. 1(a), are replaced by more uniform larger crystal grains and the rough top surface becomes flatter. The IMC layers become relatively uniform in thickness although the interface of the IMC layers with the amorphous EN becomes more crooked, implying more consumption of the EN in certain locations when forming the additional IMCs during the thermal aging.

The thickness of the Ni_3Sn_4 layer in all the aged samples was found to increase with the aging time. The average thickness was obtained for each sample by measuring the cross section area of the IMC over a certain length on the SEM image with an image analysis system and deducing a thickness value, assuming a rectangle with the same length. The results, plotted in Fig. 4 for the Sn3.5Ag vs Ni-P system, show that the IMC thickness increases linearly with $t^{½}$ and the growth rate increases with temperature. The same linear relationship is also observed for the Sn-Pb solder.

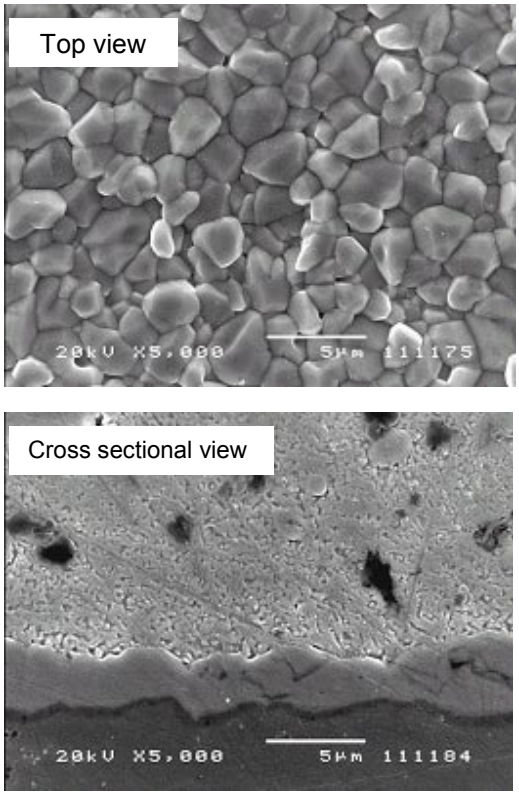

Fig. 3. Top and cross sectional views of the IMCs formed between Sn3.5Ag and NI-P UBM after 100 hours aging at 170°C.

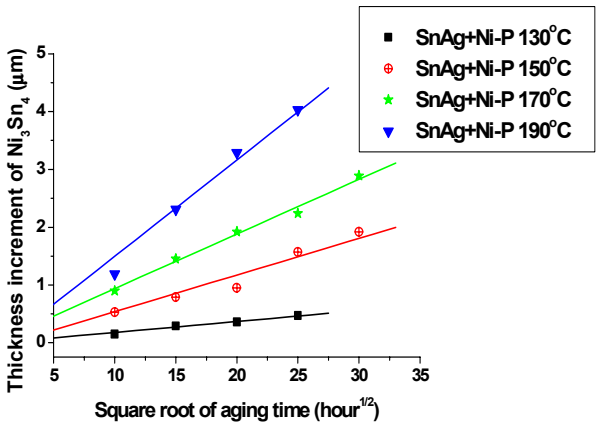

Fig. 4. Linear correlation of the IMC growth with square root of thermal aging time.

Sputtered Ni UBM. Ni_3Sn_4 intermetallic growth during thermal aging can be appreciated by the morphology change and its thickness increase. As shown in Fig. 5(a) for the Sn3.5Ag solder vs

Ni UBM, large crystal grains were formed as compared with the as reflowed ones (Fig. 2). The sputtered nickel could be consumed completely to form Ni_3Sn_4 compound. Shown in Fig. 5(b) is a cross sectional view of a Sn3.5Ag solder sample annealed for 400 hours at 190°C. About 3.8 μm of Ni3Sn4 was formed with the consumption of all the sputtered nickel. No spalling or detachment of the intermetallics from the underlying metals was observed before, and even after, the nickel was consumed.

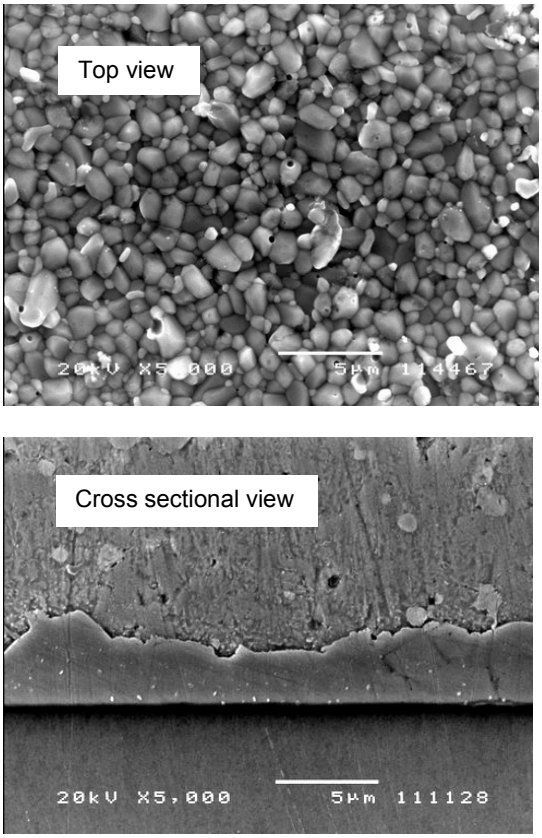

Fig. 5. Top view of the Ni_3Sn_4 of in the Sn3.5Ag vs sputtered nickel UBM system, after aging at 190°C for 400 hours.

4.3 IMC growth rate comparison

For a given UBM, (e.g., electroless Ni-P), the IMC of Sn3.5Ag solder grew faster than that of the eutectic Sn-Pb solder under the same annealing conditions, as shown in Fig. 6(a). For the same solder, e.g., Sn3.5Ag, the IMC growth rate with both types of UBM is almost the same as shown in Fig. 6(b). All the IMCs grow linearly with $t^{½}$.

Kirkendall voids. On some of the samples of the Sn3.5Ag vs Ni-P UBM, voids were observed at the interface between the Ni_3P layer and the Ni-UBM. A typical view of the voids is shown in Fig. 7. Such voids were only observed in the samples with the Ni-P UBM and aged at 170 and 190°C. The voids were found to grow with thermal aging time.

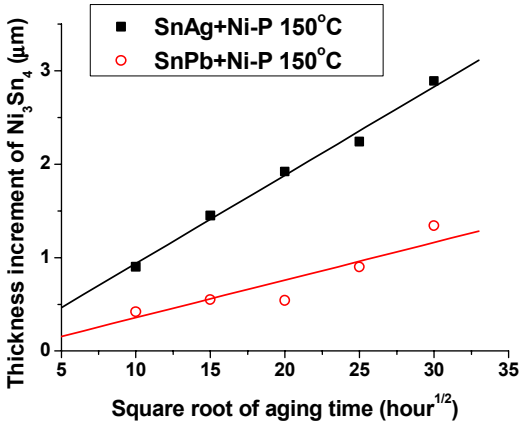

(a) Different solders with the same UBM

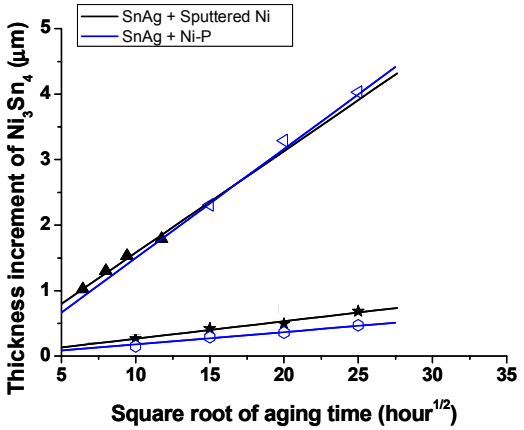

(b) Same solder with different UBMs

Fig. 6. Comparison of the IMC growth rate during thermal aging among different solder vs UBM combinations.

5 DISCUSSION

It is interesting to notice that the intermetallic compound formed at the solder/UBM interfaces in all the combination of the solders and UBMs is always Ni_3Sn_4. With the Ni-P UBM, the Ni_3Sn_4 forms on the Ni_3P, as a result of Ni depletion from and the crystallisation of the amorphous Ni-P phase [11]. By contrast, on the sputtered nickel the IMC is formed by the direct consumption of the nickel. Lead and silver in the solders are not present in the intermetallics although they are indispensable ingredient in the solder systems. Their roles in the solders are mainly to

provide all the other functionalities except adhesion to the UBMs.

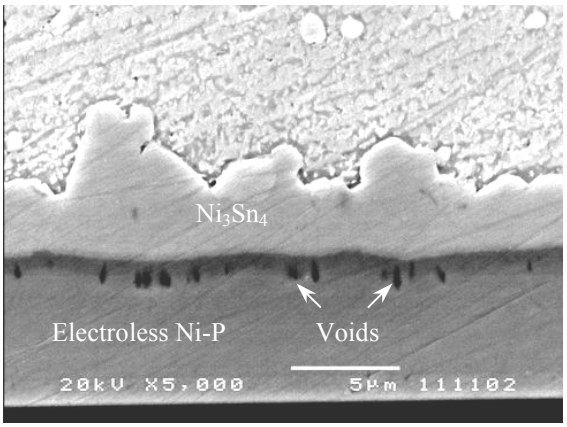

Fig. 7. Voids at the interface between Ni_3P and Ni-P UBM.

The intermetallic compound Ni_3Sn_4 is faceted in all cases studied, unlike the Cu_6Sn_5 formed between Sn-Pb solder and Cu UBM [4-5]. The latter always appears in scallop shape, which keeps the fast diffusion channel open even when there is significant intermetallic growth. It is noticed that the UBM material plays an important role in the IMC nucleation and growth, as evidenced by the clear difference in size and distribution of the IMCs. The ones formed by both Sn3.5Ag and eutectic Sn-Pb solders on electroless Ni-P UBM display a wide range of grain size distribution, while the IMCs formed on sputtered Ni UBM are very uniform in size. A notable difference between Ni-P and Ni UBMs is the formation of an additional layer of crystalline Ni_3P. The significant difference of IMC morphology as well as the slower growth rate during annealing Fig. 6(a) is believed to be due to the presence of such a layer which changes the substrate wetting as well as the diffusion channel. More work is needed to elucidate the role the element P plays in the intermetallic nucleation and growth.

Figs. 1(a) and 1(c) show many needle-like small crystals. These small grains change their morphology in prolonged reflow [13] or during additional thermal aging. By comparing Figs. 1(a) and 2(a) vs Figs. 3 and 5, one can notice the grain growth of the IMCs of the Sn3.5Ag solder related systems during the thermal aging. Similar observations were also made with the eutectic Sn-Pb solder systems. The grain growth is more obvious in the Ni-P UBM combinations. The small faceted Ni_3Sn_4 crystals could either grow bigger by incorporating additional materials or merging themselves together. Fig. 8 shows an evidence of such crystal merging during the thermal aging for the SnAg and Ni-P pair. It is reasonable to postulate that, given long enough time, the 'merging path' of the old grain boundaries (arrowed in the photo) would disappear. This is an interesting observation since the solid state coalescence of neighboring crystals would require small angle boundary between them. Under "normal" circumstance ripening has been cited as the only or dominating mechanisms for grain growth. This finding seems to suggest that there is a preferred orientation among these IMCs.

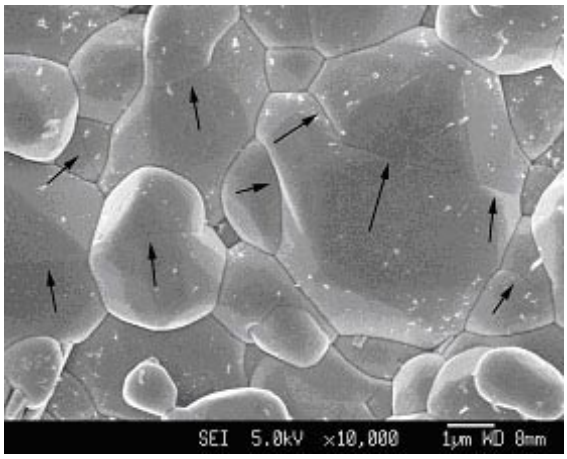

Fig. 8. Small grains merge themselves into larger grains (SnAg solder with Ni-P UBM, annealed at 190°C for 100 h. Arrows indicate the merging path of adjacent grains).

Variation in solder composition does have an effect on the growth rate of the Ni_3Sn_4 IMC during annealing. From Fig. 6(a) it is seen that the IMC of the Sn3.5Ag solder grew much faster than that of eutectic Sn-Pb solder on the same UBM. This could be attributed to the higher tin content, and thus higher chemical activity of Sn in the Sn3.5Ag solder.

The linear relation ship between the IMC thickness and $(\text{time})^{1/2}$ suggests that the IMC growth is a diffusion-controlled process. The relationship can be represented by

$$h = h_0 + k\sqrt{t} \qquad (1)$$

where h and h_0 is the thickness of the IMC at time t and zero, respectively, and k the growth rate constant. According to the classical kinetics theory, the variation of k with temperature can be represented by the Arrhenius equation

$$k = A \exp(-Q / RT) \qquad (2)$$

where A is a pre-exponential factor, T the absolute temperature and Q the activation energy of

the reaction. An Arrhenius plot, as shown in Fig. 9, is obtained for the Sn3.5Ag solder with the two types of UBM systems with the slope data from Fig. 4 and same data for the eutectic Sn-Pb solder (not shown). The activation energy for the intermetallic growth reaction is estimated as 105 KJ/mol and the pre-exponential factor *A* is 0.0697 cm^2/s.

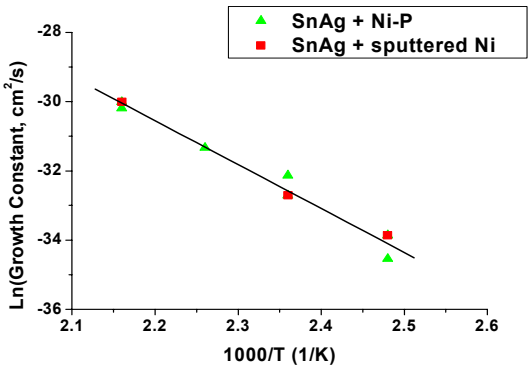

Fig. 9. Arrenius plot for the formation of IMC between SnAg3.5 solder and Ni-P and pure Ni UBMs.

The formation of the Kirkendall voids between the Ni_3P and Ni-P layers seems to be a peculiar phenomenon observed during the thermal aging process. They were observed in the samples of Sn3.5Ag solder vs Ni-P UBM system but such voids were not found at the interfaces of the sputtered nickel UBM systems. There could be two possible explanations for this. First, the thickness of the Ni layer is only 1 μm, but for the Kirkendall voids to be clearly visible under SEM, a much prolonged annealing or thicker IMC is necessary. Simple calculation shows that 1 μm of pure Ni will form about 3.8 μm of Ni_3Sn_4. Indeed in the samples that Kirkendall voids were observed, the thickness of IMC was usually more than 5 μm. Another explanation could be that the presence of the Ni_3P layer between the IMC and the UBM is a necessary condition for the void formation. At the very beginning of solder reaction the formation of Ni_3Sn_4 would deplete Ni from the surface of the electroless nickel alloy, resulting in the crystallization of the P- enriched portion of the alloy [11] to form Ni_3P. Further supply of nickel for the Ni_3Sn_4 to grow may come from two sources: decomposition of Ni_3P at the reaction front or the diffusion of nickel from the unreacted Ni-P through the Ni_3P layer. By assuming that nickel can diffuse through the Ni_3P layer easily, we may be able to explain the existence of the voids. The fast diffusion of nickel from Ni-P to the solder side would result in the enrichment of P at the interface between Ni_3P and amorphous Ni-P. If supply of nickel from the bulk Ni-P is not fast enough to 'neutralize' the extra P to form crystallized Ni_3P, a new phase of high P content and low density would be formed, which could appear as voids. Although a conclusion has not been reached, we tend to believe that the second explanation is more reasonable.

In a study on the interaction of Sn-Ag solder with Ni-P UBM during a reflow process, Jeon et al. [12, 14] found Kirkendall voids present in the Ni_3Sn_4 phase but close to a P-rich layer. They attributed the void formation to the fast diffusion of Sn from the IMC towards the Ni-P UBM and they did detect the presence of Sn in the Ni_3P layer. Other studies [11-14] under different reflow and aging conditions did not report the presence of the voids. In spite of these discrepancies, it seems reasonable to conclude that the presence and locations of the Kirkendall voids depend on a few factors or a combination of them: Ni-P UBM vs a high Sn content solder, prolonged reflow and/or long aging time at high temperatures.

Kirkendall voids used to be a serious reliability concern in the wire bonding technology. The unbalanced diffusion fluxes of aluminum and gold through the intermetallic compound phases results in the materials depletion in certain areas which affects the mechanical integrity of the wire bonds. The extend to which the Kirkendall voids in the solder vs Ni-P UBM will affect the performance and reliability of flip chip packages is not clear yet. A more systematic investigation is being carried out in the authors' labs to clarify void formation condition and their influence on the mechanical and electrical properties of solder joints.

6 CONCLUSIONS

Ni_3Sn_4 is the only Sn-containing IMC found at the interfaces of all the solder vs UBM combinations studied. On the Ni-P UBM, the IMC formed by the Sn3.5Ag solder exist in chunky crystal blocks and small crystal agglomerates, while those formed by the eutectic Sn-Pb solder exhibits similar shapes but with different sizes. On sputtered nickel UBM, the IMC of the two solder systems appear to be rather uniform fine crystals. Thermal aging results in the IMC's growth both in terms of overall thickness and crystal grain sizes. The thickness of the IMC layers in all the solder vs UBM combinations was found to increase linearly with the square root of the thermal aging time, indicating that the IMC formation reaction is a diffusion-controlled process. With the same UBM, the IMC formed by

Sn3.5Ag solder grows faster than that formed by eutectic Sn-Pb due to the higher Sn-content in Sn3.5Ag. And with the same solder, the IMC growth rate is the same on both pure nickel and Ni-P alloy. Kirkendall voids were noticed from samples of Sn3.5Ag solder vs Ni-P UBM that have undergone prolonged thermal aging at high temperature. This phenomenon warrants further study to clarify its practical implications.

7 INDUSTRIAL SIGNIFICANCE

The quantitative in formation on the IMC growth during thermal aging can serve as references in choosing appropriate UBM material and deciding their thickness for practical bumping applications. The understand on the IMC morphologies will be useful for further study on the reliability of different solder vs UBM combinations.

REFERENCES

[1] *The National Technology Roadmap for Semiconductors*, Semiconductor Industry Association, San Jose, CA, (1997).

[2] S.J. Adamson, "CSP and Flip Chip Packaging", *Advanced Packaging*, January, pp. 46-52, (2000).

[3] S. Prasad, "Technology Comparisons and the Economics of Flip Chip Packaging", *Advanced Packaging*, March, 2001, (www.apmag.com).

[4] K.N. Tu and K. Zeng, "Tin-lead (SnPb) Solder Reaction in Flip Chip Technology", *Mater. Sci. Eng.*, R34(201), pp. 1-58, (2001).

[5] K. Zeng and K.N. Tu, "Six Cases of Reliability Study of Pb-free Solder Joints in Electronic Packaging Technology", *Mater. Sci. Eng.,* R38, pp. 55-105 (2002).

[6] A. Liu, H.K. Kim, and K.N. Tu, "Spalling of Cu6Sn5 Spheroids in the Soldering Reaction of Eutectic SnPb on Cr/Cu/Au Thin Films", *J. Appl. Phys.*, Vol. 80(5), pp. 2774-2780, (1996).

[7] H.K. Kim, K.N. Tu and P.A. Totta, "Ripening-assisted Asymetric Spalling of Cu-Sn Compound Spheroids in solder Joints on Si Wafers", *Appl. Phys. Lett.*, Vol. 68(16), pp. 2204-2206, (1996).

[8] R.J.K Wassink, *Soldering in Electronics* Electrochemical Publications Ltd, pp. 173, (1984).

[9] P.G. Kim, J.W. Jang, T.Y. Lee and K.N. Tu, "Interfacial Reaction and Wetting Behavior in Eutectic SnPb Solder on Ni/Ti Thin Films and Ni Foils", *J. Appl. Phys.*, Vol. 86(12), pp. 6746-6751, (1999).

[10] J.W. Jang, D.R. Peter, T.Y. Lee and K.N. Tu, "Morphology of Interfacial Reaction between Lead-free solders and Electroless Ni-P Under Bump Metallization", *J. Appl. Phys.*, Vol. 88(11), pp. 6359-6363, (2000).

[11] J.W. Jang, P.G. Kim, K.N. Tu, D.R. Frear and P. Thompson, "Solder Reaction-Assisted Crystallization of Electroless Ni-P Under Bump Metallization in Low Cost Flip Chip Technology", *J. Appl. Phys.*, Vol. 85, pp. 8456–8463, (1999).

[12] Y.D. Jeon, K.W. Paik, K.S. Bok, W.S. Choi and C.L. Cho, "Studies on Ni-Sn Intermetallic Compound and P-rich Ni Layer at the Electroless Nickel UBM-Solder Interface and their Effects on Flip Chip Solder Joint Reliability", *201 Electronic Components and Technology Conference, IEEE,* 2001.

[13] M. Gunawan, M. He, Z. Chen and G. Qi, "Morphology study of intermetallic compound between lead-free solders and electroless Ni-P UBM", *1st International Conference on Materials Processing for Properties and Performance,* Singapore, August 2002.

[14] Y.D. Jeon, K.W. Paik, K.S. Bok, W.S. Choi and C.L. Cho, "Studies of Electroless Nickel Under Bump Metallurgy – Solder Interfacial Reactions and Their Effects on Flip Chip Solder Joint Reliability", *J. Electronics Materials*, Vol. 31, pp. 520-528 (2002).